

Two-Step Seismic Noise Reduction Saused by COVID-19 Induced Reduction in Social Activity in Metropolitan Tokyo, Japan

Suguru Yabe (✉ s.yabe@aist.go.jp)

National Institute of Advanced Industrial Science and Technology <https://orcid.org/0000-0002-5614-0198>

Kazutoshi Imanishi

National Institute of Advanced Industrial Science and Technology

Kiwamu Nishida

Earthquake Research Institute, the University of Tokyo

Full paper

Keywords: Seismic noise, Cultural noise, COVID-19, Tokyo

Posted Date: July 28th, 2020

DOI: <https://doi.org/10.21203/rs.3.rs-48413/v1>

License:  This work is licensed under a Creative Commons Attribution 4.0 International License.
[Read Full License](#)

Version of Record: A version of this preprint was published on November 4th, 2020. See the published version at <https://doi.org/10.1186/s40623-020-01298-9>.

Abstract

The COVID-19 pandemic that started at the end of 2019 forced populations around the world to reduce social and economic activities; it is believed that this can prevent the spread of the disease. In this paper, we report a seismic noise analysis during such an induced social activity reduction taking the Tokyo Metropolitan area, Japan. Using seismic data obtained from 18 stations in the Metropolitan Seismic Observation Network (MeSO-net), a two-step seismic noise reduction in the frequency bands 1–20 Hz and 20–40 Hz was observed during the timeline of COVID-19 in Tokyo. The first noise reduction occurred at the beginning of March in the frequency band 20–40 Hz. This corresponded with the request of the Prime Minister of Japan for a nationwide shutdown of schools. Although social activity was not reduced significantly at this juncture, local reduction of seismic wave excitation in the high frequency band, 20–40 Hz, was recorded at some MeSO-net stations located in school properties. The second reduction of seismic noise occurred at the end of March to the beginning of April 2020 in the frequency band 1–20 Hz. This timing corresponds to when the Governors of the Tokyo Metropolitan area requested citizens to stay home and when the state of emergency was declared for the Tokyo Metropolitan area by the government, respectively. The estimated population at train stations abruptly dropped since this timing, which suggests that social activity was severely reduced. Such large-scale change in social activity affects the seismic noise level in the low frequency bands. The seismic noise level started to increase from the middle of May correlating with increase in population at the train stations. This suggests that social activity restarted even before the state of emergency was lifted at the end of May. The two-step seismic noise reduction observed in this study has not been reported in other cities around the world. Unexpected reduction of social activity due to COVID-19 provided us a rare opportunity to investigate the characteristics of seismic noise caused by human activities.

1. Introduction

Seismic stations record seismic signals from many sources. For example, a large “noise” called a microseism occurs in the frequency band 0.05–1 Hz because of interactions between the solid earth and meteorological and oceanic phenomena (e.g., Longuet-Higgins 1950; Hasselmann 1963). Conversely, seismic noise in the frequency band higher than 1 Hz is known to show diurnal variability, where a high noise level is recorded during daytime (e.g., Bonnefoy-Claudet et al. 2006). This is called cultural noise or anthropogenic noise, as it is known to be excited by human activities such as transportation and machine vibrations (e.g., Gutenberg 1958; Asten 1978; Asten and Henstridge 1984).

The COVID-19 pandemic began at the end of 2019 in China and spread throughout the world (Andersen et al. 2020). To prevent the spread of the disease, reduction in social activity was practiced around the world (e.g., Tian et al. 2020). Earlier observations have indicated that the seismic noise level decreases during long holidays such as Christmas and New Year holidays (Okada and Obara 2000). Seismic noise level reduction corresponding to social activity reduction for COVID-19 management has been reported in some cities (Poli et al. 2020; Xiao et al. 2020; Lindsey et al. 2020). Social activity reduction is rare, and hence, its occurrence due to COVID-19 enables seismologists to understand the characteristics of cultural

noise. Seismic noise reduction recorded by seismometers in Italy and China were correlated with mobility data of people in the corresponding cities (Poli et al. 2020; Xiao et al. 2020) suggesting that transportation is the principal noise source. Seismic monitoring with distributed acoustic sensing revealed more detailed spatial changes in social activities in Palo Alto City, California, USA (Lindsey et al. 2020). The study showed that the amount of traffic noise reduction in the city depends on the characteristics of the districts. A district near a grocery store showed a ~50 % reduction in noise, whereas a district near a hospital showed only a minimal reduction. The amount of seismic noise reduction varies among the cities as the COVID-19 situation and the social response to it vary (Xiao et al. 2020). Hence, it is important to accumulate observations at various cities to understand the characteristics of cultural seismic noise in urban environments.

This study reports seismic noise reduction caused by social activity reduction for COVID-19 management in the Tokyo Metropolitan area. The Metropolitan Seismic Observation Network (MeSO-net), which consists of more than 300 seismic stations, functions in Tokyo and the surrounding prefectures (Sakai and Hirata 2009) (Figure 1). MeSO-net stations are settled at the bottom of shallow (10–20 m) boreholes, usually located in schools or public park properties. They are close to the ground surface and thus, more susceptible to seismic waves caused by human activities (Kasahara et al. 2009) than the High Sensitivity Seismograph Network (Hi-net), which are often used in the seismic analysis for small earthquakes at a depth of 100 m depth or more (Okada et al. 2004; Obara et al. 2005). Kawakita and Sakai (2009) reported various cultural noises observed in MeSO-net stations. They showed that the background noise level is higher in the central Tokyo Metropolitan area, which is attributed to high levels of social activities there. They also analyzed running spectra of seismic records in MeSO-net stations and found a high noise level of about 50 Hz. This noise, according to them, is excited by vibrations of machines such as motors and inverters, which use electrical power supply with a frequency of 50 Hz. They also documented cultural noise excited by trains and cars. Train signals were observed between 5:00 h and 0:00 h with the busiest period at 7:00 h to 9:00 h, corresponding to work commuting time. Strong car signals are observed at MeSO-net stations close to elevated highways. The amount of such cultural noise was expected to decrease because of the social activity reduction during COVID-19 management.

We monitored the temporal changes in the seismic noise level in MeSO-net stations and compared the changes with the timeline of COVID-19 in the Tokyo Metropolitan area. We applied polarization analysis (Park et al. 1987) to continuous seismic records of MeSO-net stations to investigate the temporal variations in seismic noise characteristics. We report a two-step seismic noise reduction in different frequency bands correlated with timelines of COVID-19, which was not observed in other cities (Poli et al. 2020; Xiao et al. 2020; Lindsey et al. 2020). We explain the timeline of COVID-19 in Tokyo in Section 2. Seismic data and polarization analyses are explained in Section 3. We define the average seismic noise level of each station prior to the COVID-19 pandemic in Section 4. Temporal variations of seismic noise relative to the average noise level are discussed in Section 5. Section 6 presents a summary.

2. Timeline Of Covid-19 In The Tokyo Metropolitan Area

The COVID-19 disease spread into regions of Japan in January 2020. The first case of COVID-19 in Japan was reported on January 16, 2020. The first case in Tokyo was reported on January 24, 2020 (Figure 2). The daily reported number of confirmed new COVID-19 cases was low until February; it started increasing from the beginning of March. The daily reported number exceeded 100 around the beginning of April and it reached its maximum around the middle of April. It started decreasing gradually toward the end of May, though it again started increasing later.

To deal with this pandemic situation, gradual social activity reduction was requested by the local and national governments. The first step of social activity reduction in Tokyo occurred when the Prime Minister of Japan requested a nationwide shutdown of schools. At this stage, only primary, junior high, and high schools were shut down, though all other economic activities continued. School shutdown began on March 2, 2020 (A in Figure 2) and this was enforced until the beginning of June. As the situation worsened, the Governor of the Tokyo metropolitan area requested citizens to stay at home on March 26, 2020 (B in Figure 2). A state of emergency was declared by the national government on April 7, 2020 for the Tokyo metropolitan area (C in Figure 2) and for entire Japan on April 16, 2020. We note that the declaration of the state of emergency in Japan did not enforce lockdown of cities and did not legally confine citizens to their homes; it just requested them to stay indoors voluntarily. As the daily reported number of confirmed new COVID-19 cases decreased, the state of emergency in the Tokyo metropolitan area was lifted on May 25, 2020 (D in Figure 2). Although social distancing is being continuously requested by governments, the daily reported number of confirmed new COVID-19 cases is gradually increasing again after the emergency was lifted.

We referred population data to understand how people reacted to the requests for social activity reduction by governments during the timeline of COVID-19 in Tokyo. Population data were published by Agoop Corp. on their website. The population data were estimated using GPS location information collected from smartphones. Figure 3 shows the estimated populations around train stations near the studied MeSO-net stations. The locations of the train stations are shown in Figure 1b. At each location, the number of people located within a radius of 300 m or 500 m around the train station was counted every day considering the weight of their staying time within the region.

Population data show that the number of people around the train stations in the Tokyo Metropolitan area decreased abruptly at two timings. A small drop occurred when the schools were closed on March 2, 2020. A larger drop in population occurred at the end of March to the beginning of April when the Governor of the Tokyo Metropolitan area requested citizens to stay at home and a state of emergency was declared. By the end of April, the population decreased to $\frac{1}{2}$ – $\frac{3}{4}$ of the population in January, which shows that social activity was significantly reduced after the declaration of a state of emergency in the Tokyo Metropolitan area. However, this reduction in population did not continue for a long time. After the long holidays at the beginning of May, which is called the “Golden Week” in Japan, the population started increasing, even though the emergency was not lifted. Although the daily reported number of confirmed new COVID-19 cases kept increasing, the population continued to increase around the train stations until the end of June, when it recovered to $\frac{1}{2}$ – $\frac{3}{4}$ of the level in January.

3. Seismic Data And Methods

We used continuous seismic records of the MeSO-net stations from January 1, 2018 to June 30, 2020. Although MeSO-net consists of more than 300 stations, we selected only 18 stations situated in the middle of the Tokyo Metropolitan area (Figure 1). Table 1 shows the MeSO-net stations considered in this study and the types of public property that are present above the seismometers. These MeSO-net stations have servo accelerometers, which have a flat sensitivity to the DC component with a 200-Hz sampling rate. Of these 18 stations presented in Table 1, six stations (E.AYHM, E.KHDM, E.HN1M, E.SBAM, E.SBCM, and E.HGCM) show a two-step seismic noise reduction, whereas the other stations except for one station (E.MYMM) show one-step seismic noise reduction. In this manuscript, we mainly present the results of four stations: two as examples of the two-step reduction (E.HN1M and E.SBCM) and the other two as examples of the one-step reduction (E.IKBM and E.NSJM). The results pertaining to the remaining 14 stations are presented in the Supplementary Material.

We applied the polarization method (Park et al. 1987) to three-component continuous seismic records. We used 2-s moving time windows with 50% overlap to calculate the Fourier spectra covariance matrix. We took an average of the complex matrixes every hour to stabilize the analysis. Then, we calculated the eigen values and eigen vectors of the averaged complex matrixes. As the covariance matrix is a Hermitian matrix, all eigen values are real. Incident azimuth and incident angle of polarization were calculated along with the phase differences between two horizontal components and between the horizontal and vertical components from the complex eigen vector for the maximum eigen value.

Table 1 List of MeSO-net stations considered in this study

Name	Latitude	Longitude	Ground surface facility
E.HN1M	35.62165	139.71629	Elementary school
E.SBCM	35.84169	139.68864	Junior high school
E.SBAM	35.65107	139.75020	Elementary school
E.AYHM	35.67264	139.71544	High school
E.KHDM	35.71281	139.73606	Elementary school
E.HGCM	35.82589	139.75708	Junior high school
E.IKBM	35.73725	139.70917	Elementary school
E.NSJM	35.68669	139.68708	Elementary school
E.GNZM	35.66521	139.76473	Junior high school
E.HYHM	35.83756	139.72761	High school
E.YYIM	35.71855	139.76035	The University of Tokyo
E.ENZM	35.60844	139.70786	Elementary school
E.TKMM	35.63993	139.73456	Junior high school
E.RYGM	35.69324	139.79560	Elementary school
E.YKKM	35.70734	139.80654	Elementary school
E.TYPM	35.70483	139.71339	Park
E.KYNM	35.86361	139.81531	Park
E.MYMM	35.88994	139.77272	Elementary school

4. Average Noise Level

To discuss the temporal changes in the seismic noise level, we first defined the average noise level. As the cultural noise level changes by the day of the week and hour in a day (e.g., Okada and Obara 2000; McNamara and Buland 2004; Marzorati and Bindi 2006; Groos and Ritter 2009), the average noise level needs to be defined every hour and every day of the week. This study uses data from January 1, 2018 to January 31, 2020, during which time the COVID-19 pandemic was not severe in Japan. The average noise levels were defined for each component by the median value of the square root of the corresponding trace element of the averaged Fourier spectra covariance matrix. Holiday periods such as national holidays, year-end and new-year holidays, and summer holidays, were removed from the calculation of the average noise level because the noise level on such days is expected to be lower compared with the

usual activity periods. Figure 4 and Figure S1 show the average noise level of the Up-Down (UD) component during a week.

Although the average noise level and its temporal variations vary among the MeSO-net stations, we find several common characteristics. Large noise levels are observed at around 4 Hz throughout a week, though it becomes lower on a Sunday. Figure 5 compares the noise level of all the studied stations at 4 Hz on Monday and Sunday. On Monday, many stations have a noise peak at 5:00 h. As Kawakita and Sakai (2009) observed, this timing corresponds to when the train service starts. The high noise level also continues between 9:00 h and 16:00 h, which corresponds to working time. A drop in noise level is observed at many stations during lunch break. On Sunday, the daytime noise level is much lower than that of the weekday. Although noise level increases around 5:00 h, prominent noise peaks are not observed. It is interesting to note that the noise level difference between Monday and Sunday is almost the same among all the stations. This suggests that the seismic noise wavefield of cultural noise at this frequency, excited by social activity on weekdays, is common in the central Tokyo Metropolitan area, even though the background noise level is different among the stations.

The second prominent characteristic is that large noise signals are also observed at a frequency band of 10–20 Hz. Figure 6 compares the noise level of all the studied stations at 13 Hz on Monday and Sunday. The noise level is also lower on Sunday, as it is in the case of 4 Hz. On Monday, noise peaks around 5:00 h observed at 4 Hz are less evident at this frequency band. The high noise level during daytime is observed on both Monday and Sunday. Noise level difference between a weekday and Sunday is smaller at 13 Hz than it is in 4 Hz, though its temporal variations are not common among the stations. This suggests that the seismic wavefield of cultural noise excited on weekdays in this frequency band reflect more local social activities around the stations.

5. Temporal Noise Level Variations

We monitored temporal variations of seismic noise level during 2.5 years between January 1, 2018 and June 30, 2020. To evaluate temporal variations clearly, we calculated the noise reduction ratio, which is defined as the seismic noise level (square root of the trace element of the averaged Fourier spectra covariance matrix) divided by the average noise level of the corresponding day of the week and hour. Here, holiday periods such as national holidays, year-end and new year holidays, and summer holidays are treated as Sunday. Figures 7 and S2 show temporal variations for noise reduction ratio of UD components as well as the incident azimuth of noise polarization estimated by polarization analysis.

Temporal variations of noise reduction ratio in Figures 7 and S2 show that the noise level varies throughout the 2.5 years, even before the COVID-19 pandemic influenced social activities. There seems to be seasonal variations in the noise reduction ratio. Winter season (December to February) tends to show a higher noise level in many stations, which is especially evident in E.IKBM, E.SBCM (Figure 7), and E.RYGM (Figure S2). This high noise level is often observed in the frequency range of > 20 Hz. Summer

season (around August) also shows a higher noise level in some stations (for example, E.HN1M (Figure 7), E.SBAM, and E.YKKM (Figure S2)).

Although noise reduction ratio shows temporal variations, the incident azimuth and incident angle of noise polarization is constant with time suggesting that spatial distributions of noise sources are common for 2.5 years. However, there are several examples where the incident azimuth changes abruptly or gradually with time. For example, a large noise level was observed from April to October in 2018 and 2019 at E.HGCM station (Figure S2). Incident azimuth changes abruptly when the large noise level started and ended. In this case, the incident azimuth for the low and high noise periods is stable with time, which suggests that spatial distributions of the cultural noise sources around the station change seasonally.

Noise reduction ratio in 2020 shows a completely different pattern from that in 2018 and 2019 at many stations. The low noise period abruptly started around April at many stations. This low noise level spans only limited frequency bands such as 1–40 Hz at some stations (for example, E.HN1M), whereas it spans the entire frequency band at other stations (for example, E.IKBM). Although low noise periods are also observed in 2018 and 2019, the noise level in the low-frequency band of 1–20 Hz is not reduced significantly in 2018 and 2019. The amount of cultural noise in a low-frequency band (around 1–10 Hz) excited on weekdays are common among MeSO-net stations (Figure 5), whereas that in the higher frequency band is different (Figure 6). This suggests that cultural noise in a lower frequency band records large-scale social activity in the Tokyo Metropolitan area, whereas cultural noise in the higher frequency band records local social activity around the stations. Therefore, the seismic noise reduction in the lower frequency band that occurred in 2020 is interpreted to be due to the social activity reduction for COVID-19 in the Tokyo Metropolitan area.

At several stations (E.HN1M, E.SBCM, E.AYHM, E.KHDM, E.SBAM, and E.HGCM), seismic noise reduction in a high frequency band of 20–40 Hz or 20–50 Hz precedes seismic noise reduction in the low frequency band of 1–20 Hz. We calculated the median noise reduction ratio in two different frequency bands (5–10 Hz and 25–35 Hz) during daytime (10:00 h to 16:00 h) (Figures 8 and S3). The seismic noise reduction in the high frequency bands occurred when the schools were closed at the beginning of March. As the MeSO-net stations are usually installed in school properties, social activity reduction in a school building decreases seismic wave excitation there, which is recorded in the seismometers at the high frequency bands that is sensitive to the locally excited cultural noise. However, this first-step noise reduction was recorded only in limited stations. The relative strength of cultural noise sources around the stations in the higher frequency bands may determine whether seismic noise reduction in the school buildings can be observed.

The seismic noise level started recovering since May 2020. At many stations, the noise reduction ratio increased after the Golden Week at the beginning of May in both frequency bands (Figures 7, 8, S2, and S3). This recovery correlates well with the population recovery (Figure 3). It started before the state of emergency was lifted on May 25, 2020, which suggests that social activity was restarted before the government officially announced the relaxation.

6. Summary

This study reports seismic noise reduction in the Tokyo Metropolitan area associated with social activity reduction for COVID-19. Although seismic noise reduction associated with the lockdown of cities has already been reported at cities in Italy and China, the MeSO-net stations in the Tokyo Metropolitan area show different temporal patterns in which seismic noise is reduced in two stages correlating with the timeline of COVID-19 in Japan. The first reduction occurred in the frequency band of 20 Hz and higher at the beginning of March when schools were closed. The second reduction occurred in the frequency band of 1–20 Hz from the end of March to the beginning of April when the Governor of the Tokyo Metropolitan area requested citizens to stay at home and when the state of emergency was declared. Many people stopped commuting and social activity was severely reduced at that time. After the middle of May, social activity was gradually restarted, and the seismic noise level increased again.

Two-step noise reduction in different frequency bands is a unique characteristic observed in the MeSO-net. When schools were closed at the beginning of March, social activities in the school properties were locally reduced, though social activities in the entire Tokyo Metropolitan area were not severely reduced. As many MeSO-net stations are settled in school properties, local reductions of seismic wave excitation in them were recorded in the high-frequency bands (above 20 Hz). However, noise reduction in this step was observed only in a limited number of stations. If social activities around the stations are high and if the principal noise source in this frequency band is different from the schools, the first step of noise reduction would not be observed. On the other hand, when the state of emergency was declared at the beginning of April, social activities in the entire Tokyo Metropolitan area were reduced. Such wide-scale reduction in seismic wave excitation was recorded in the lower frequency band (1–20 Hz). Irregular cultural noise reduction in the Tokyo Metropolitan area due to social activity reduction for COVID-19 showed that the spatial extent of the social activities that affect seismometers is wider for the lower frequency noise.

Declarations

Data Availability

MeSO-net data are available at the Hi-net website (<https://www.hinet.bosai.go.jp/?LANG=en>). Data for confirmed COVID-19 cases in Tokyo were taken from the website of the Tokyo Metropolitan government (<https://stopcovid19.metro.tokyo.lg.jp/cards/number-of-confirmed-cases/>). Population data are published by Agoop Corp. on their website (https://corporate-web.agoop.net/pdf/covid-19/agoop_analysis_coronavirus.pdf).

Competing interests

The authors declare that they have no competing interests.

Funding

This study was supported by the management expense account of the National Institute of Advanced Industrial Science and Technology (AIST).

Authors' contributions

All authors contributed toward the conception of this study. SY analyzed data and drafted the manuscript. All authors contributed to the revision and approved the final version of the manuscript.

Acknowledgement

We used the Python package of Obspy (Beyreuther et al. 2010) to analyze the seismic wave data.

References

1. Andersen KG, Rambaut A, Lipkin WI, Holmes EC, Garry RF (2020) The proximal origin of Sars-Cov-2. *Nat Med* 26:450– doi: 10.1038/s41591- 020-0820-9.
2. Asten MW (1978) Geological control of the three-component spectra of Rayleigh-wave microseisms. *Bull Seism Soc Am* 68:1623–
3. Asten MW, Henstridge JD (1984) Arrays estimators and the use of microseisms for reconnaissance of sedimentary basins. *Geophysics* 49:1828–
4. Beyreuther M, Barsch R, Krischer L, Megies T, Behr Y, Wassermann J (2010) ObsPy: A Python Toolbox for Seismology. *Seism Res Let* 81(3):530-533. doi:10.1785/gssrl.81.3.530.
5. Bonnefoy-Claudet S, Cotton F, Bard P-Y (2006) The nature of noise wavefield and its applications for site effects studies: A literature review. *Earth Sci Rev* 79:205– doi:10.1016/j.earscirev.2006.07.004.
6. Groos JC, Ritter JRR (2009) Time domain classification and quantification of seismic noise in an urban environment. *Geophys J Int* 179:1213– doi:10.1111/j.1365-246X.2009.04343.x.
7. Gutenberg B (1958) Microseisms. *Advances in Geophysics* 5:53–
8. Hasselmann K (1963) A statistical analysis of the generation of microseisms. *Rev Geophys* 1:177– doi:10.1029/RG001i002p00177.
9. Kasahara K, Sakai S, Morita Y, Hirata N, Tsuruoka N, Nakagawa S, Nanjo K, Obara K (2009) Development of the Metropolitan Seismic Observation Network (MeSO-net) for detection of megathrust beneath Tokyo metropolitan area. *Bull Earthquake Res Inst Univ Tokyo* 84:71–
10. Kawakita Y, Sakai S (2009) Various Types of Noise in MeSO-net. *Bull Earthquake Res Inst Univ Tokyo* 84:127–
11. Lindsey N, Yuan S, Lellouch A, Gualtieri L, Lecocq T, Biondi B (2020) City-scale dark fiber DAS measurements of infrastructure use during the COVID-19 pandemic. arXiv preprint, arXiv:2005.04861.
12. Longuet-Higgins MS (1950) A theory of the origin of microseisms. *Philos Trans R Soc London Ser A* 243:1– doi:10.1098/rsta.1950.0012.

13. Marzorati S, Bindi D (2006) Ambient noise levels in north central Italy. *Geochem Geophys Geosyst* 7:Q09010. doi:10.1029/2006GC001256.
14. McNamara DE, Buland RP (2004) Ambient Noise Levels in the Continental United States. *Bull Seism Soc Am* 94:1517– doi:10.1785/012003001.
15. Obara K, Kasahara K, Hori S, Okada Y (2005) A densely distributed high-sensitivity seismograph network in Japan: Hi-net by National Research Institute for Earth Science and Disaster Prevention. *Rev Sci Instrum* 76:021301. doi:10.1063/1.1854197.
16. Okada Y, Obara K (2000) Ground noise levels at high sensitivity seismic stations in the Kanto-Tokai region, central Japan. *Rep Natl Res Inst Earth Sci Disas Resilience* 60:15–
17. Okada Y, Kasahara K, Hori S, Obara K, Sekiguchi S, Fujiwara H, Yamamoto A (2004) Recent progress of seismic observation networks in Japan -Hi-net, F-net, K-NET and KiK-net -. *Earth Planets Space* 56: xv–xxviii, doi:10.1186/BF03353076.
18. Park J, Vernon FL, Lindberg CR (1987) Frequency dependent polarization analysis of high-frequency seismograms. *J Geophys Res* 92:12664– doi:10.1029/JB092iB12p12664.
19. Poli P, Boaga J, Molinari I, Cascone V, Boschi L (2020) The 2020 coronavirus lockdown and seismic monitoring of anthropic activities in Northern Italy. *Scientific Reports* 10:9404. doi:10.1038/s41598-020-66368-0.
20. Sakai S, Hirata N (2009) Distribution of the Metropolitan Seismic Observation network. *Bull Earthquake Res Inst Univ Tokyo* 84:57–
21. Tian H, Liu Y, Li Y, Wu CH, Chen B, Kraemer MU, Li B, Cai J, Xu B, Yang Q, Wang B (2020) An investigation of transmission control measures during the first 50 days of the COVID-19 epidemic in China. *Science* 368(6491):638– doi:10.1126/science.abb6105.
22. Xiao H, Eilon C, Ji C, Tanimoto T (2020) COVID-19 societal response captured by seismic noise in China and Italy. *arXiv preprint arXiv:2005.00131*.

Figures

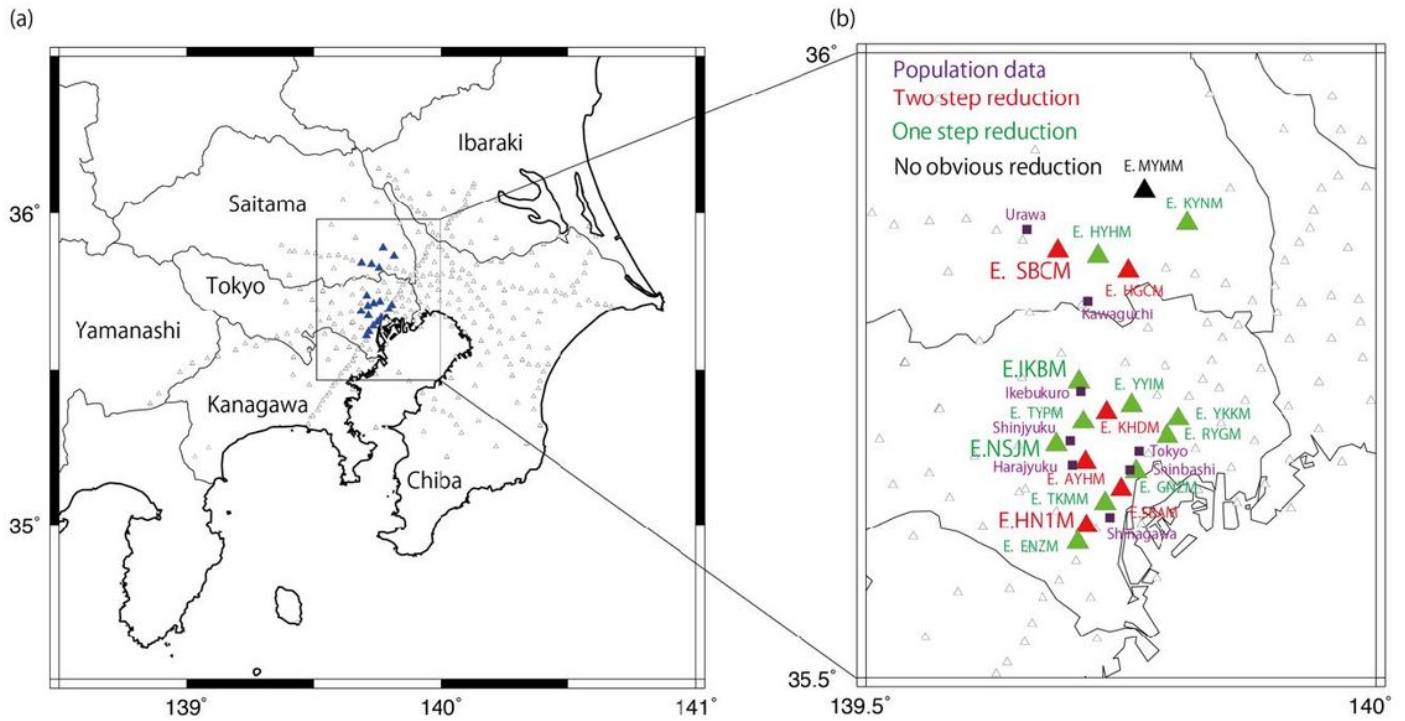
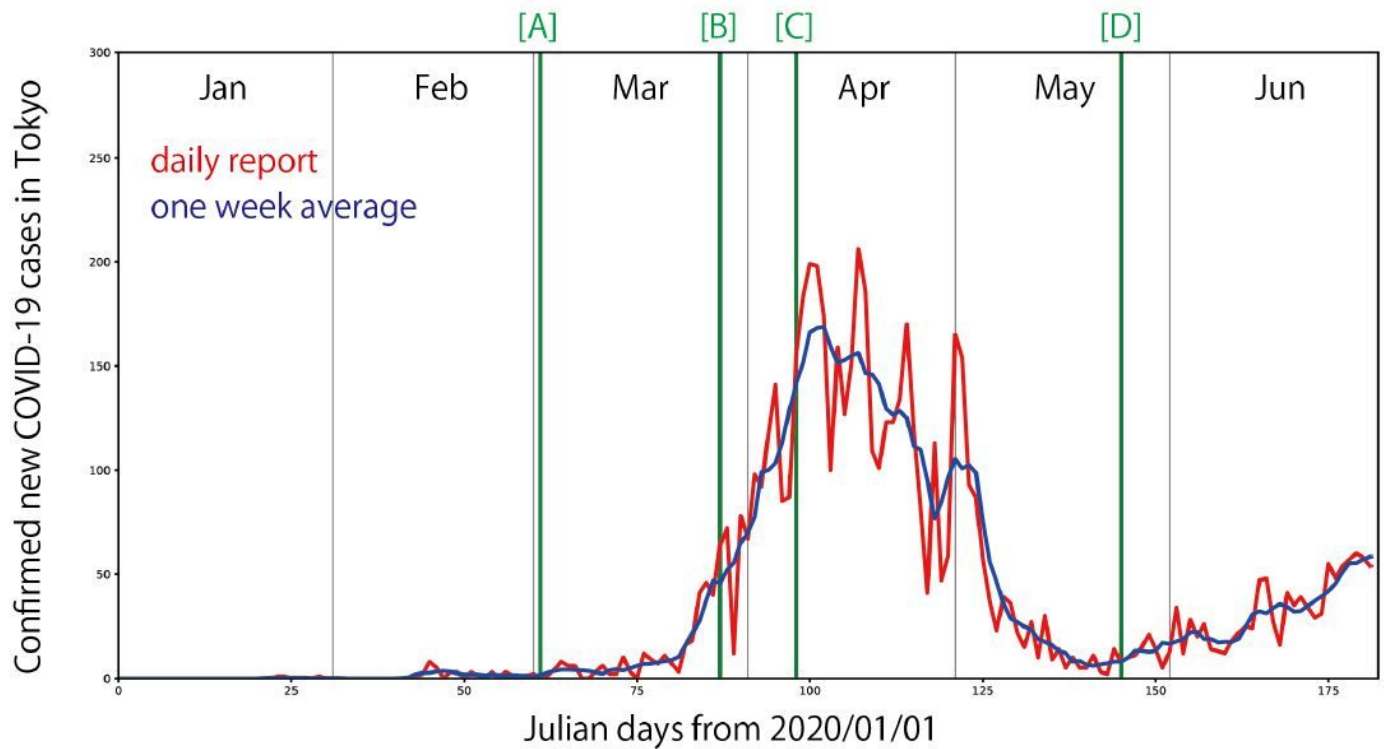


Figure 1

Location map of stations in the MeSO-net in the Tokyo Metropolitan area. (a) Map of Kanto region of Japan. Triangles show MeSO-net stations. Blue triangles are the MeSO-net stations considered in this study. (b) Close-up map in the middle of the Tokyo Metropolitan area. Red, green, and black triangles show the style of noise reduction observed in this study. Purple squares are train stations for which population data are presented in Figure 3.



Social response to COVID 19 in Tokyo
 [A] School shutdown
 [B] The Governor's request to stay at home
 [C] State of emergency declared in Tokyo
 [D] State of emergency lifted in Tokyo

Figure 2

Timeline of COVID-19 in Tokyo. The red curve shows the daily reported number of confirmed new COVID-19 cases in Tokyo. The blue curve is smoothed using a 1-week time window. Green lines indicate the timing of government actions for COVID-19.

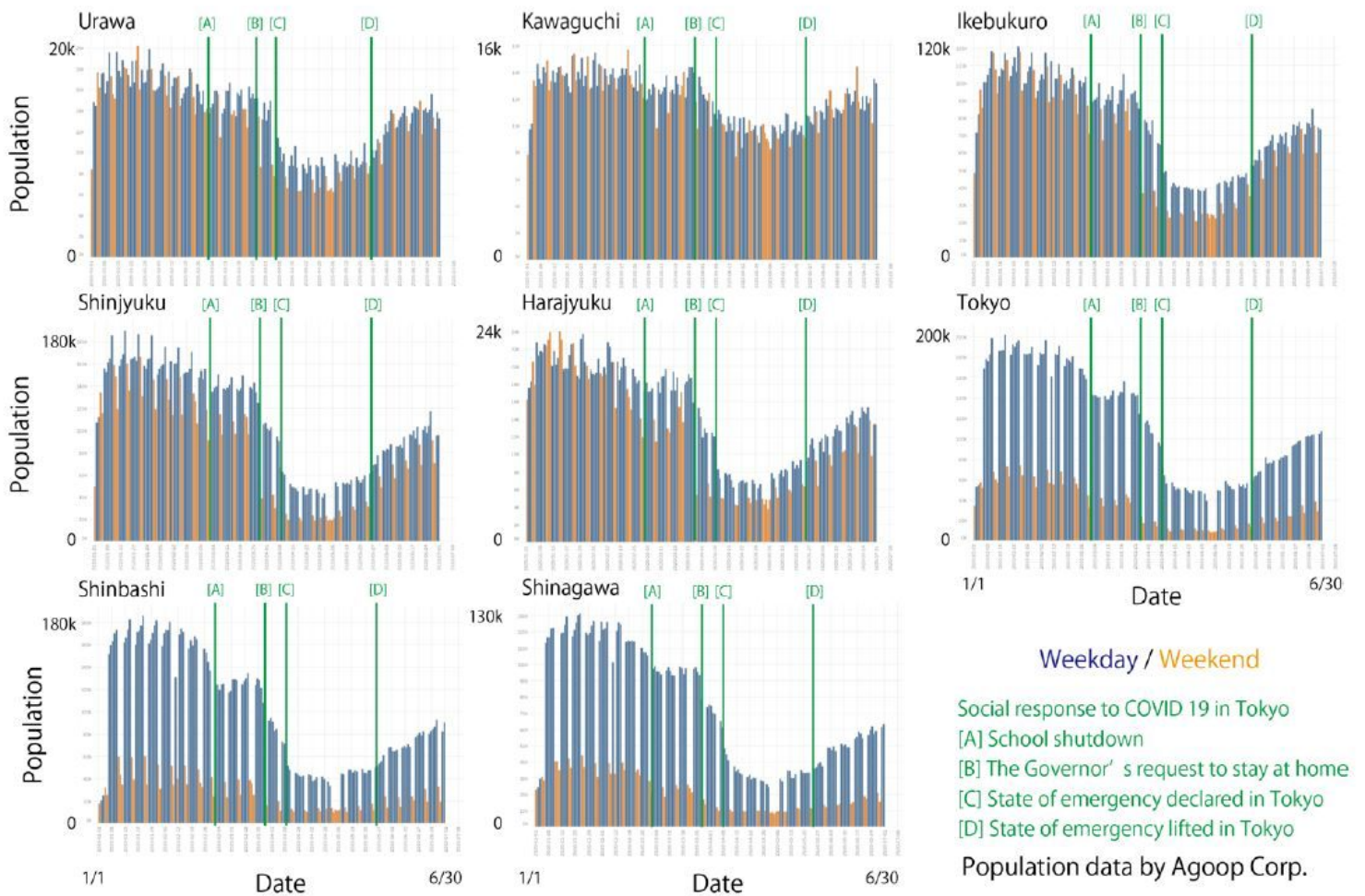
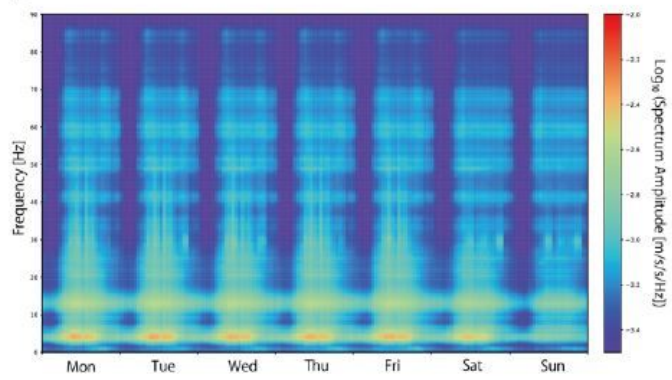


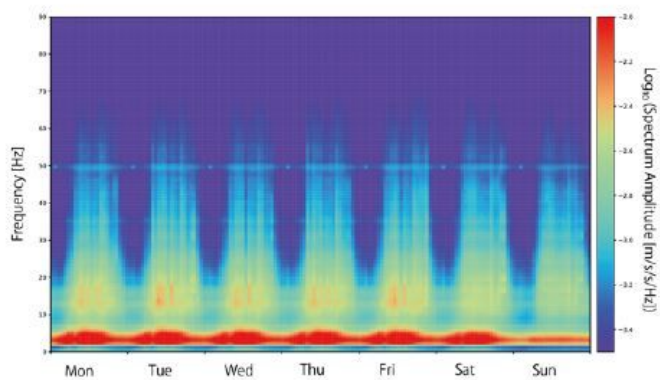
Figure 3

Population at the train stations around MeSO-net stations. Population data were provided by Agoop Corp. This figure is modified from figures originally published by Agoop Corp. on their website (https://corporate-web.agoop.net/pdf/covid-19/agoop_analysis_coronavirus.pdf; accessed on 1 July 2020) with their permission. Blue and orange bars represent daily population around stations for weekdays and weekend days, respectively. Green lines represent timings of government actions for COVID-19.

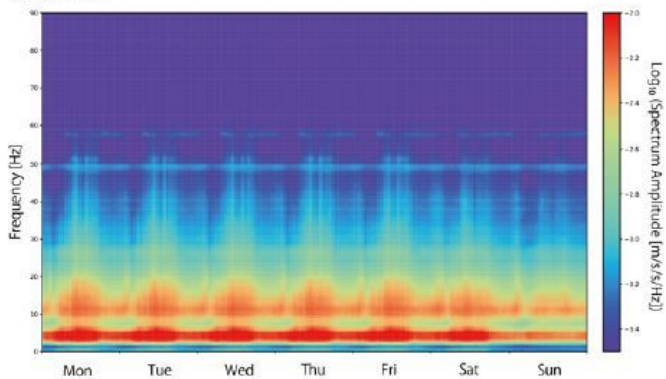
(a) E.HN1M



(b) E.SBCM



(c) E.IKBM



(d) E.NSJM

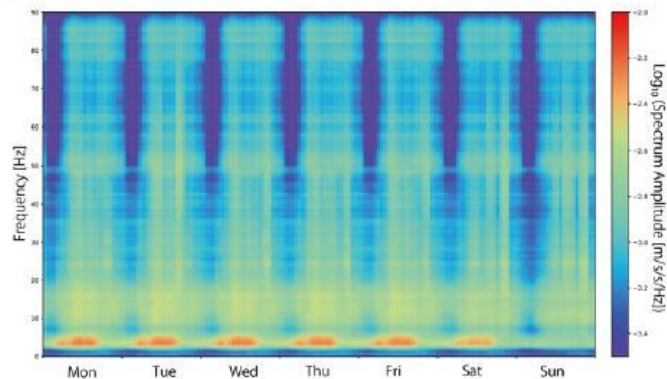


Figure 4

Average noise level of UD components at four stations.

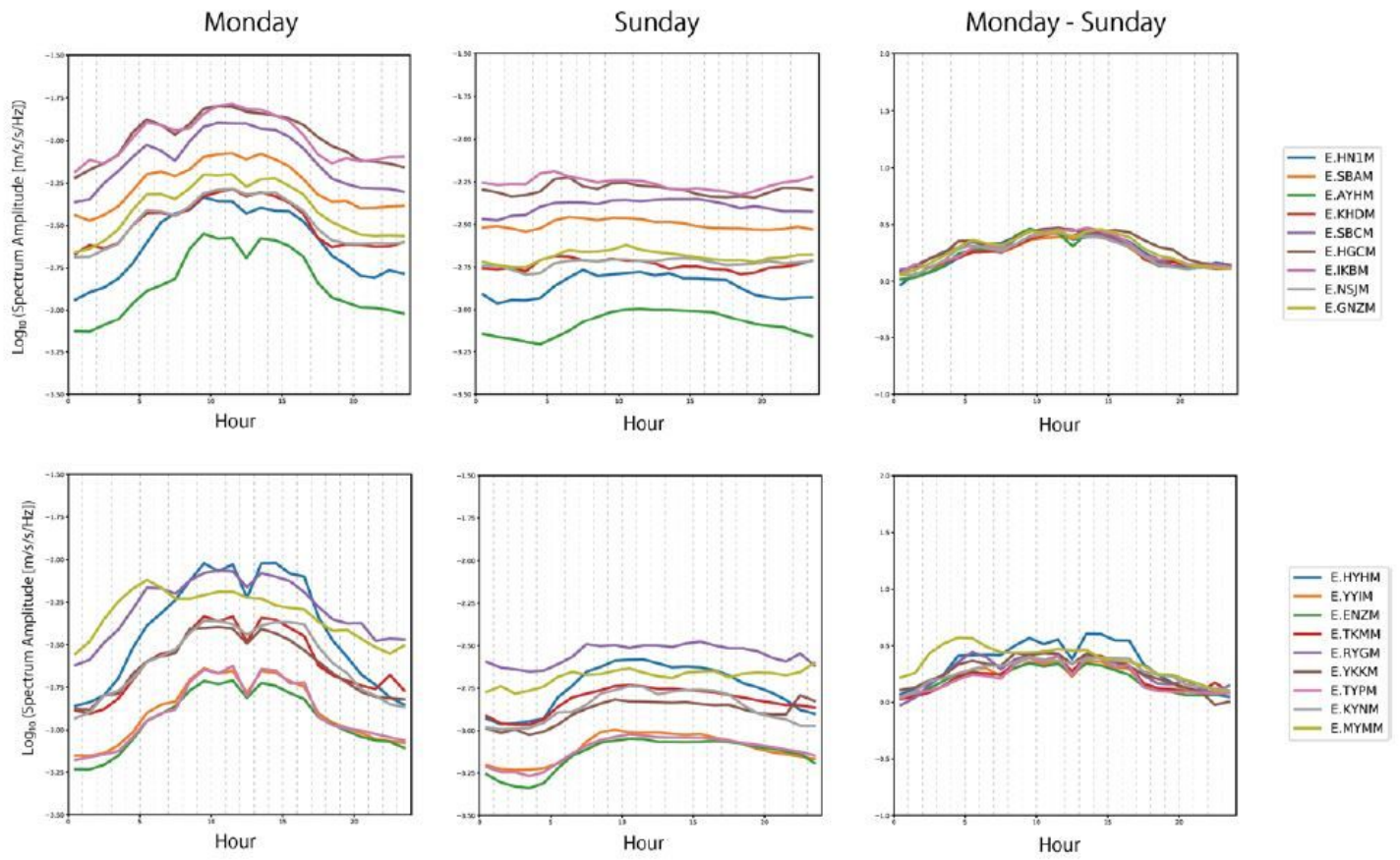


Figure 5

Noise level at 4 Hz on Monday and Sunday. (left) On Monday. (middle) On Sunday. (right) Differences between Monday and Sunday.

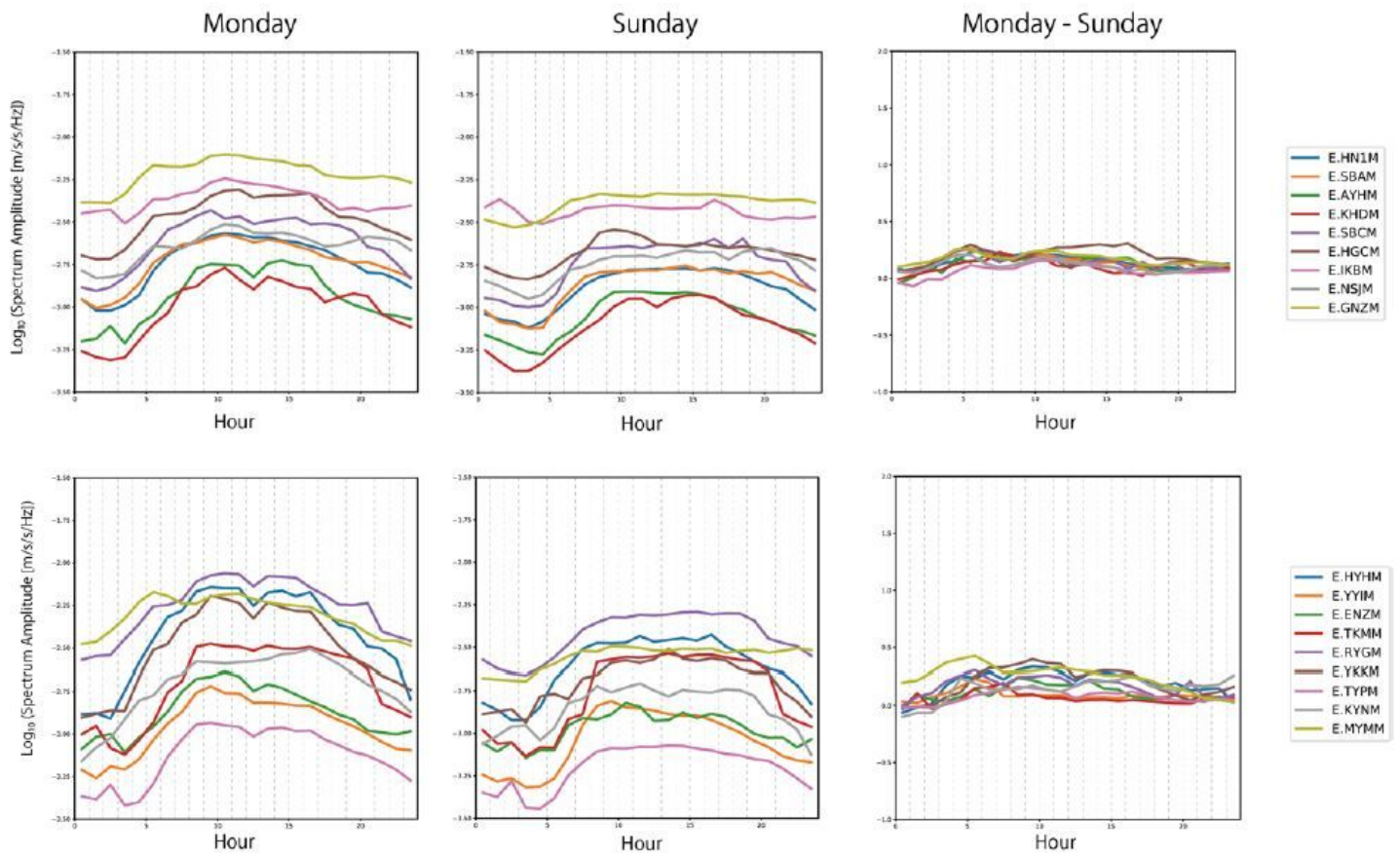


Figure 6

Noise level at 13 Hz on Monday and Sunday. (left) On Monday. (middle) On Sunday. (right) Differences between Monday and Sunday.

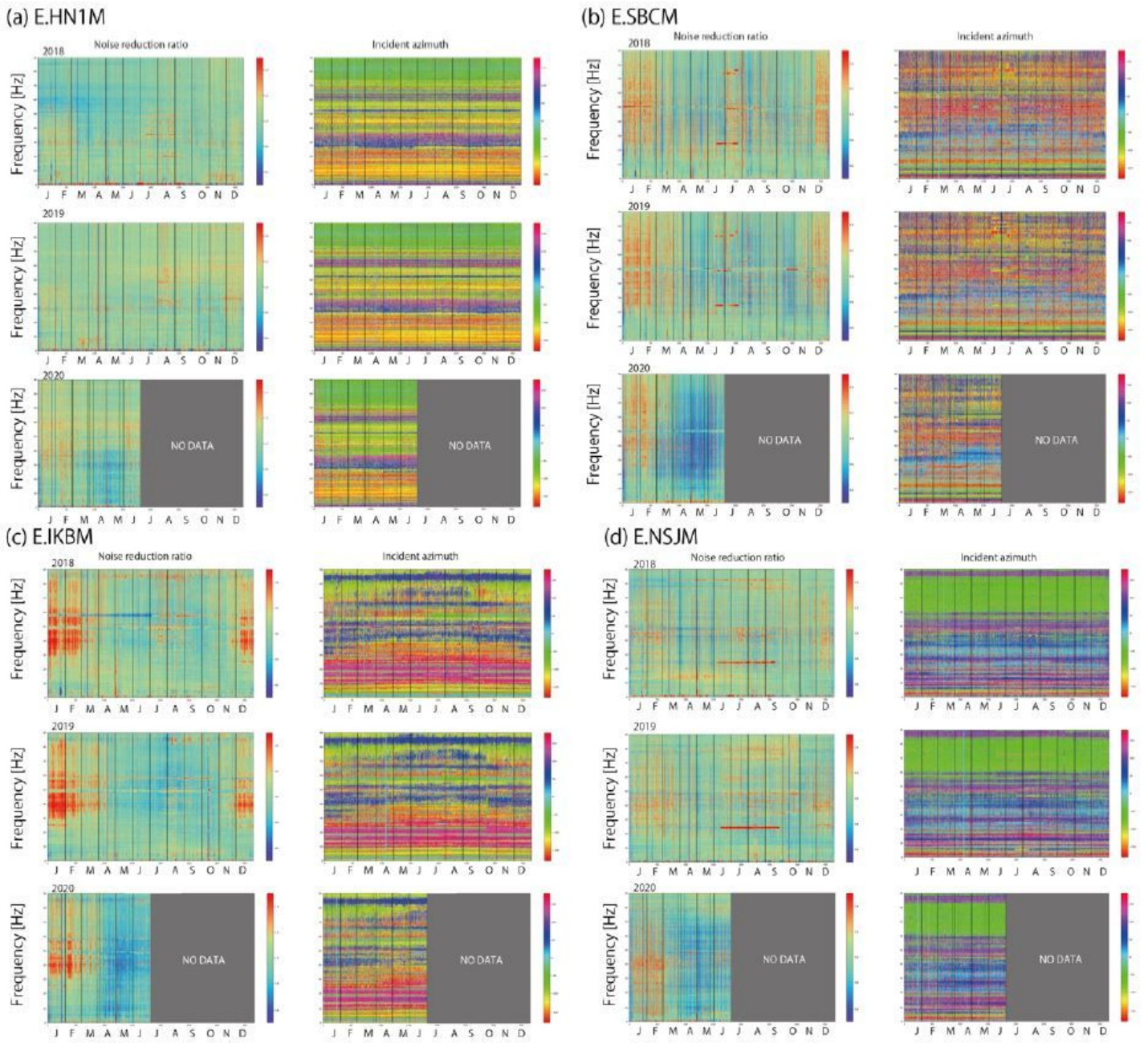


Figure 7

Noise reduction ratio of UD components and incident azimuth of noise polarization at four stations. The cases of two-step (a and b) and one-step seismic noise reduction (c and d).

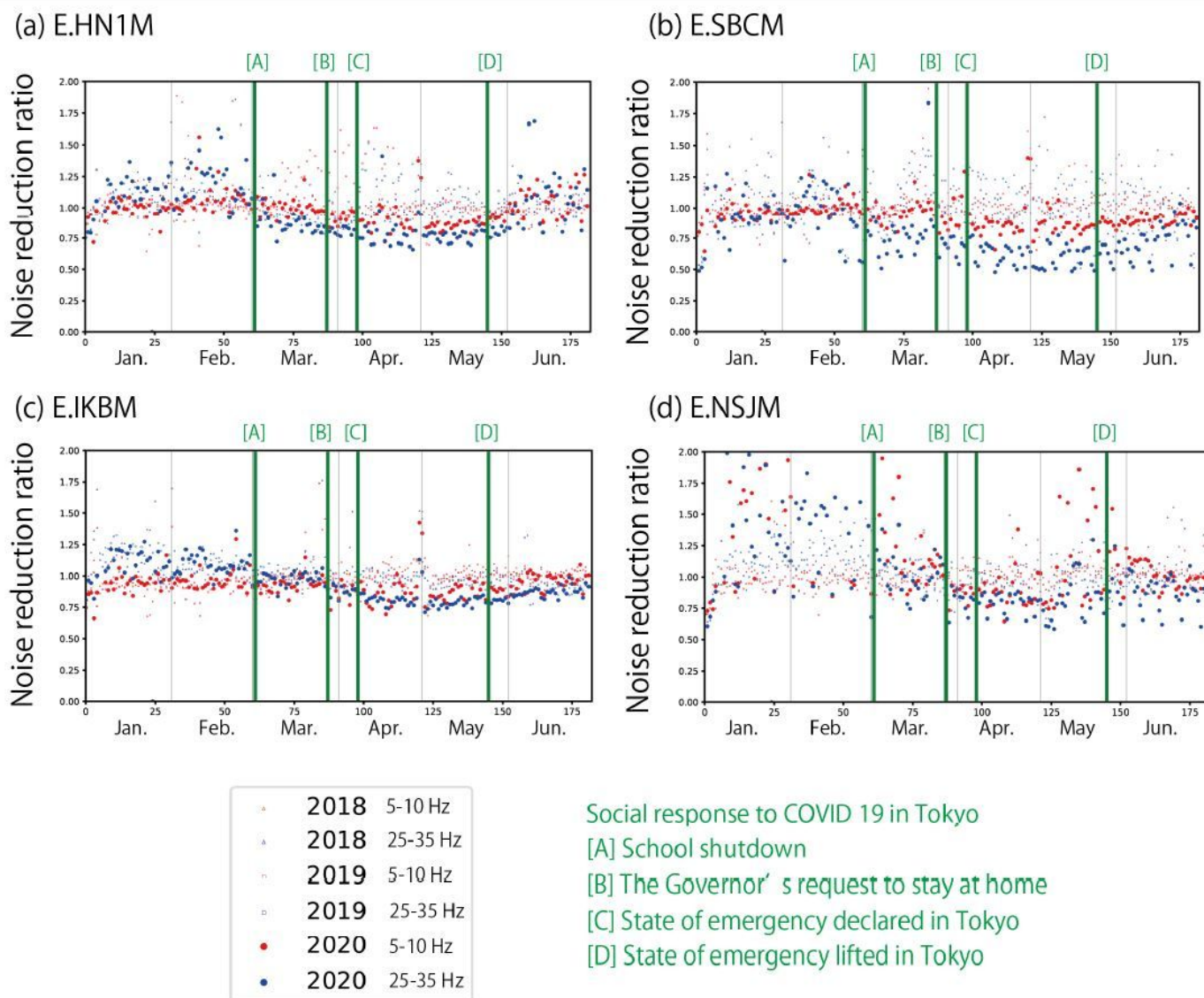


Figure 8

Median noise reduction ratio during daytime in two different frequency bands at four stations.

Supplementary Files

This is a list of supplementary files associated with this preprint. Click to download.

- [FigA.png](#)
- [Supp.pdf](#)